Electronic Supplementary Material (ESI) for Dalton Transactions.
This journal is © The Royal Society of Chemistry 2018

Electronic Supplementary Information for

Two MOFs as dual-responsive photoluminescence sensors for metal and inorganic ions detection

Zhong–Jie Wang, Fa-Yuan Ge, Guo-Hao Sun and He-Gen Zheng*

State Key Laboratory of Coordination Chemistry, School of Chemistry and Chemical Engineering, Collaborative Innovation Center of Advanced Microstructures, Nanjing University, Nanjing 210023, P. R. China

Crystal structure determination

The crystal structures were determined by single-crystal X-ray analyses. Data collections were performed using a Bruker Apex Smart CCD diffractometer with Mo-Kα radiation with an φ–ω mode (λ = 0.71073 Å). The structures were solved with direct methods using the SHELXTL program[1-2] and refined anisotropically with SHELXTL using full-matrix least-squares procedures. Crystallographic data and structural refinements parameters for these compounds are given in Table S1. Selected bond lengths and angles are listed in Table S2. Hydrogen-Bonding geometry is listed in Table S3.

Table S1. Crystal data and structural refinements parameters of **1** and **2**.

Compound	**1**	**2**
Empirical formula	$C_{26}F_4H_{15}N_5O_4Zn$	$C_{29}F_4H_{24}N_6O_6Cd$
Formula weight	602.80	740.94
Crystal system	Triclinic	Monoclinic
Space group	$P\bar{1}$	*C2/c*
a / Å	10.8391(8)	17.7736(18)
b / Å	11.1144(9)	17.8696(18)
c / Å	11.6293(9)	18.3763(19)
α / °	116.6100(10)	90.00
β/ °	91.5160(10)	98.7620(10)
γ/ °	103.2240(10)	90.00
V / Å^3	1205.92(16)	5768.3(10)
Z	2	8
D_{calcd} / g cm^{-3}	1.660	1.706
μ / mm^{-1}	1.095	0.839
F(000)	608	2976
θ min-max / °	1.952, 27.559	1.626, 28.247
Tot., uniq. data	11076, 5576	26942, 7143
R(int)	0.0254	0.0397
Observed data [$I > 2\sigma(I)$]	5576	7143
Nres, Npar	0, 365	7, 427
R_1, wR_2 [$I > 2\sigma(I)$][a]	0.0341, 0.0794	0.0383, 0.0858
GOF on F^2	1.039	1.079
Min. and max resd dens (e ·Å^{-3})	-0.359, 0.378	-0.756, 0.962

[a]"R_1"=$\Sigma||F_o|-|F_c||/|\Sigma|F_o|$. "$wR_2$"=$\{\Sigma[w(F_o^2-F_c^2)^2]/\Sigma[w(F_o^2)^2]\}^{1/2}$; where $w=1/[\sigma^2(F_o^2)+(aP)^2+bP]$, $P=(F_o^2+2F_c^2)/3$.

Table S2. Selected bond lengths (Å) and angles (deg) for **1** and **2**.

		1	
N(1)-Zn(1)	1.9889(17)	N(5)-Zn(1)[a]	2.0030(17)
O(1)-Zn(1)	1.9509(14)	O(3)-Zn(1)	1.9568(15)
O(1)-Zn(1)-O(3)	97.46(6)	O(1)-Zn(1)-N(1)	112.46(6)
O(3)-Zn(1)-N(1)	118.71(7)	O(1)-Zn(1)-N(5)[a]	111.14(6)
O(3)-Zn(1)-N(5)[a]	104.75(7)	N(1)-Zn(1)-N(5)[a]	111.39(7)
		2	
Cd(1)-N(4)	2.270(3)	Cd(1)-N(1)	2.272(3)
Cd(1)-O(3)	2.319(2)	Cd(1)-O(1W)	2.330(2)
Cd(1)-O(2)[b]	2.406(2)	Cd(1)-O(2)	2.422(2)
O(2)-Cd(1)[b]	2.405(2)	N(4)-Cd(1)-N(1)	176.58(9)
N(4)-Cd(1)-O(3)	92.52(9)	N(1)-Cd(1)-O(3)	90.53(9)
N(4)-Cd(1)-O(1W)	86.22(9)	N(1)-Cd(1)-O(1W)	92.44(9)
N(1)-Cd(1)-O(1W)	92.44(9)	O(3)-Cd(1)-O(1W)	86.12(8)
N(4)-Cd(1)-O(2)[b]	89.98(8)	N(1)-Cd(1)-O(2)[b]	92.03(8)
O(3)-Cd(1)-O(2)[b]	81.03(7)	O(1W)-Cd(1)-O(2)[b]	166.42(7)
N(4)-Cd(1)-O(2)	86.75(8)	N(1)-Cd(1)-O(2)	91.28(8)
O(3)-Cd(1)-O(2)	152.11(7)	O(1W)-Cd(1)-O(2)	121.59(7)
O(2)[b]-Cd(1)-O(2)	71.10(7)		

Symmetry codes:
for **1 :** a = $x + 2, -y, -z + 1$.
for **2 :** b = $-x + 1, y, -z + 1/2$.

Table S3. Hydrogen-Bonding Geometry (Å,°) for **1** and **2**.

D−H···A	d(D···A)	∠D−H···A
	1	
N3-H3A···O4[a]	2.880(2)	158(2)
	2	
N3-H3A···O1W[a]	2.936(3)	141.2
O1W-H1WA···O5	2.781(4)	178.1
O1W-H1WB···O3	3.174(3)	125.6
O1W-H1WB···O4	2.569 (5)	139.6
O1W-H1WB···O4'	2.744(7)	178.0

Symmetry codes:

for **1:** a = $x, y - 1, z - 1$.

for **2:** a = $x, -y + 2, z + 2/1$.

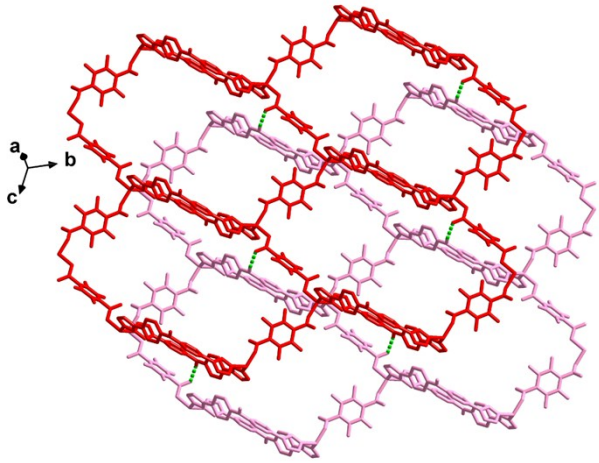

Fig. S1 Schematic representation of H-bonding interactions in **1**. The H-bonding interactions are shown with green dash lines.

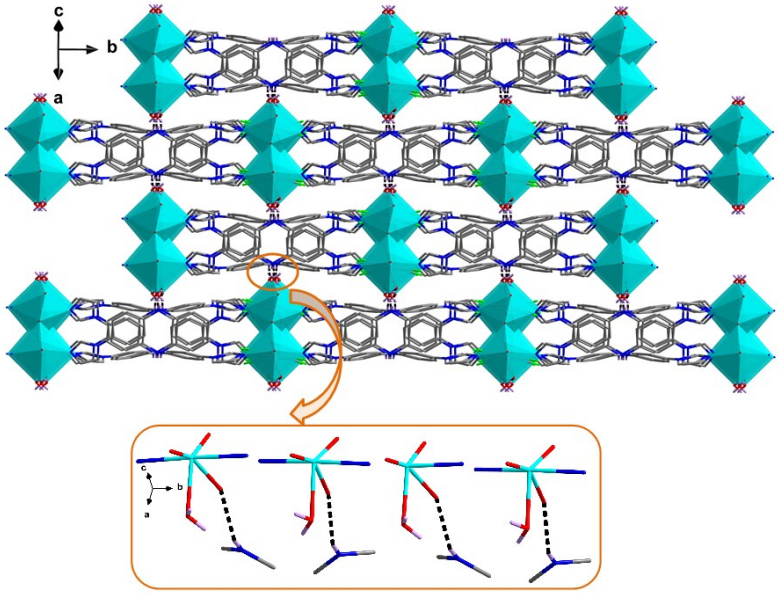

Fig. S2 Schematic representation of H-bonding interactions in **2**. The H-bonding interactions are shown with balck dash lines.

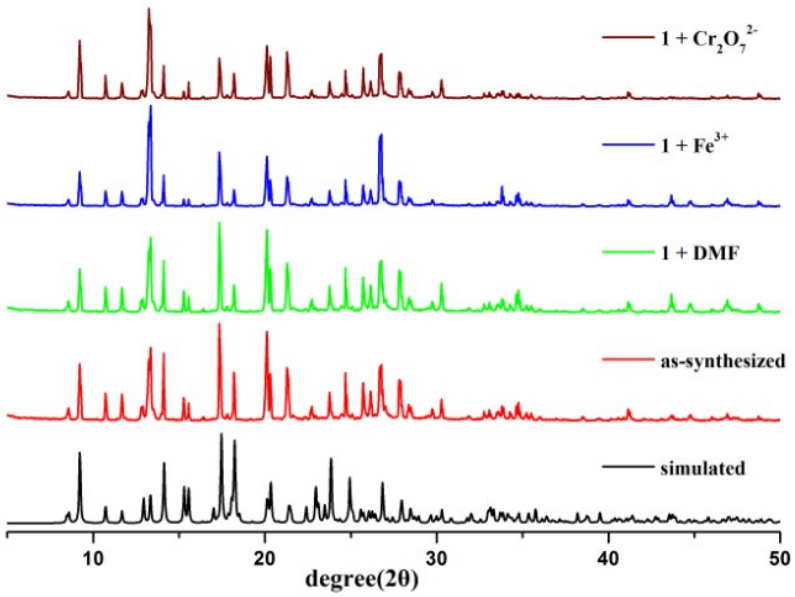

Fig. S3 Powder X-ray diffraction patterns of **1**.

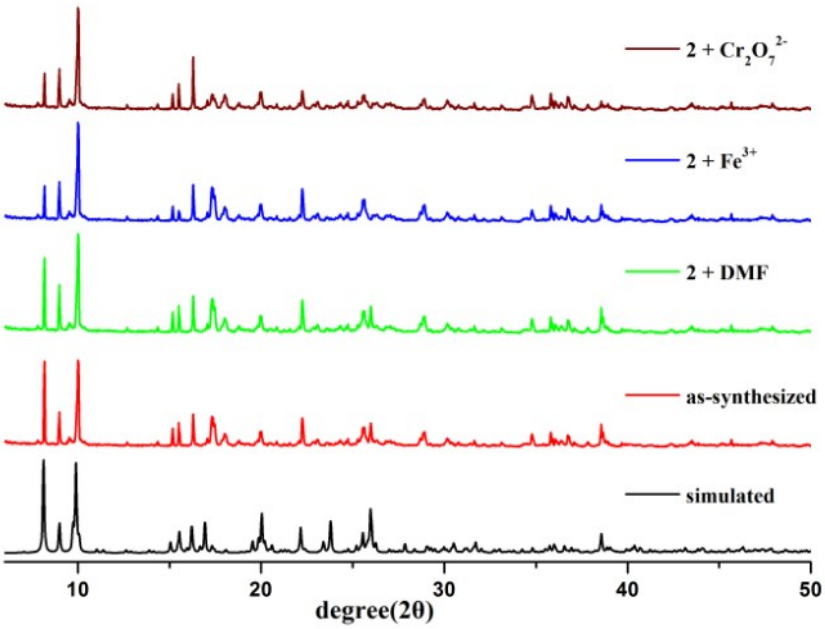

Fig. S4 Powder X-ray diffraction patterns of **2**.

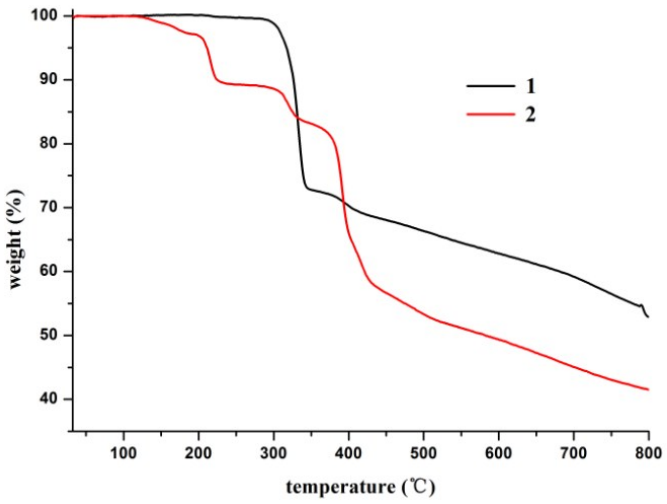

Fig. S5 TGA plots of **1** and **2**.

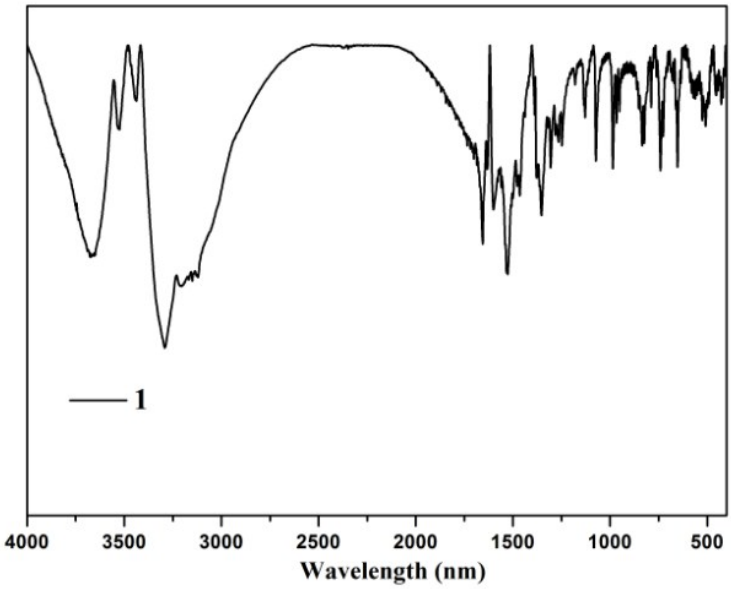

Fig. S6 IR spectra of **1**.

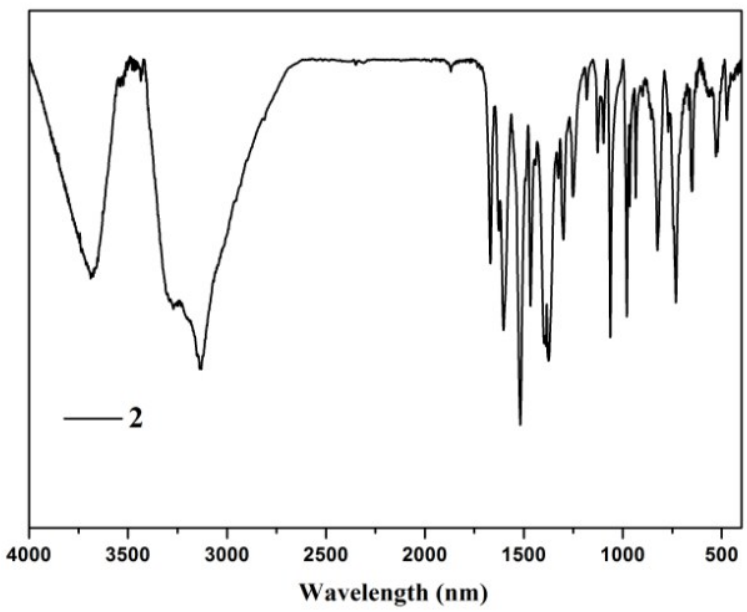

Fig. S7 IR spectra of **2**.

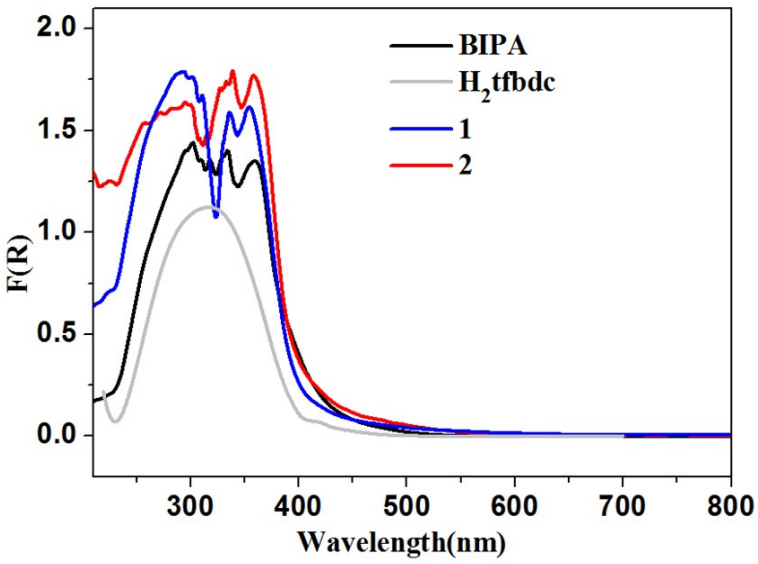

Fig. S8 Solid-state UV−vis absorption spectra of BIPA ligand, H_2tfbdc ligand, **1** and **2**.

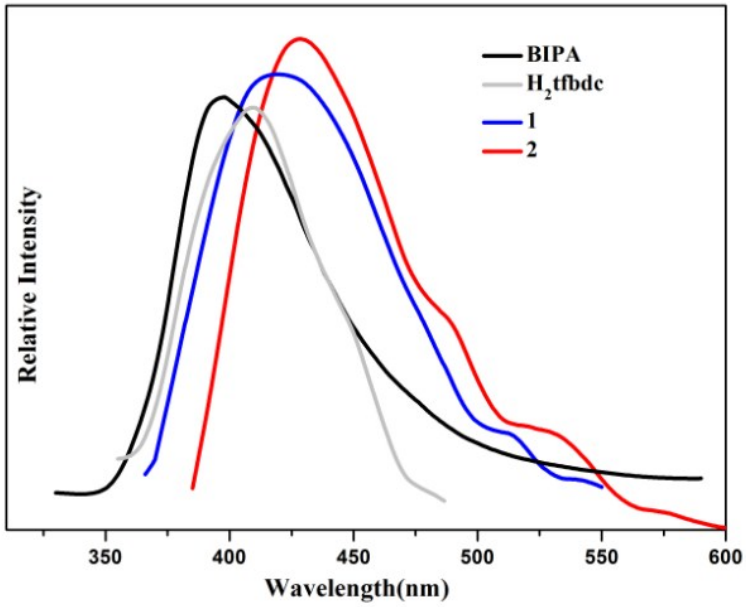

Fig. S9 Solid-state photoluminescent spectra of BIPA ligand, H_2tfbdc ligand, **1** and **2** (λ_{ex} 300 nm).

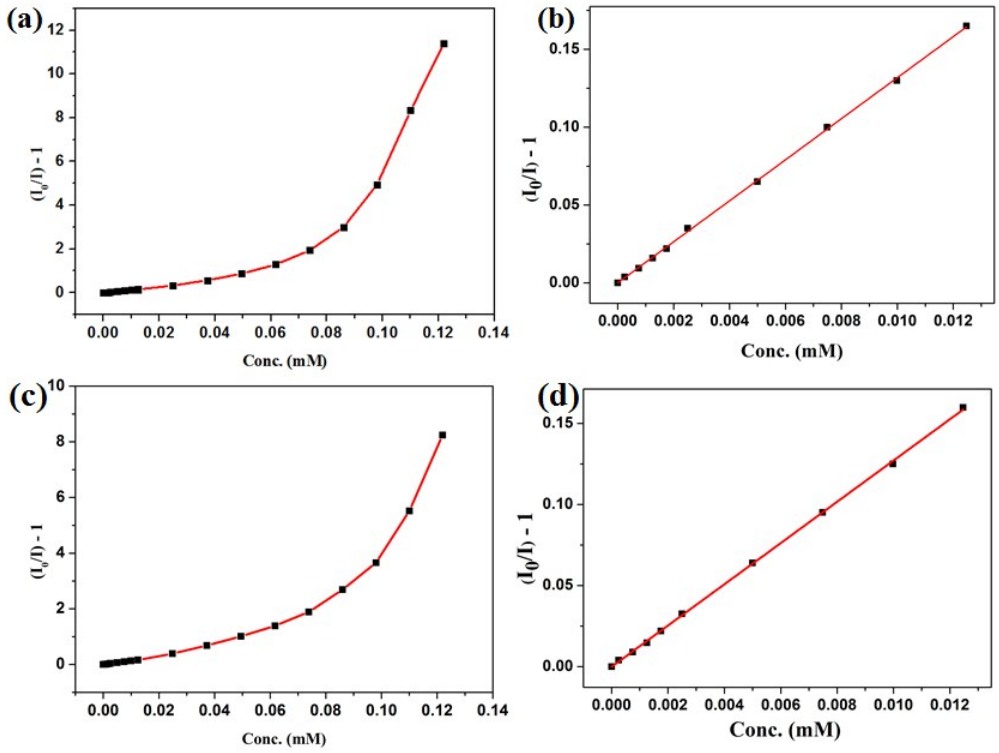

Fig. S10 (a) SV curve for **1** by gradual addition of Fe^{3+} ion (50 μL, 5 × 10^{-3} M) in DMF. (b) Emission quenching linearity relationship at low concentrations of Fe^{3+} ion for **1**. (c) SV curve for **2** by gradual addition of Hg^{2+} ion (50 μL, 5 × 10^{-3} M) in DMF. (d) Emission quenching linearity relationship at low concentrations of Hg^{2+} ion for **2**.

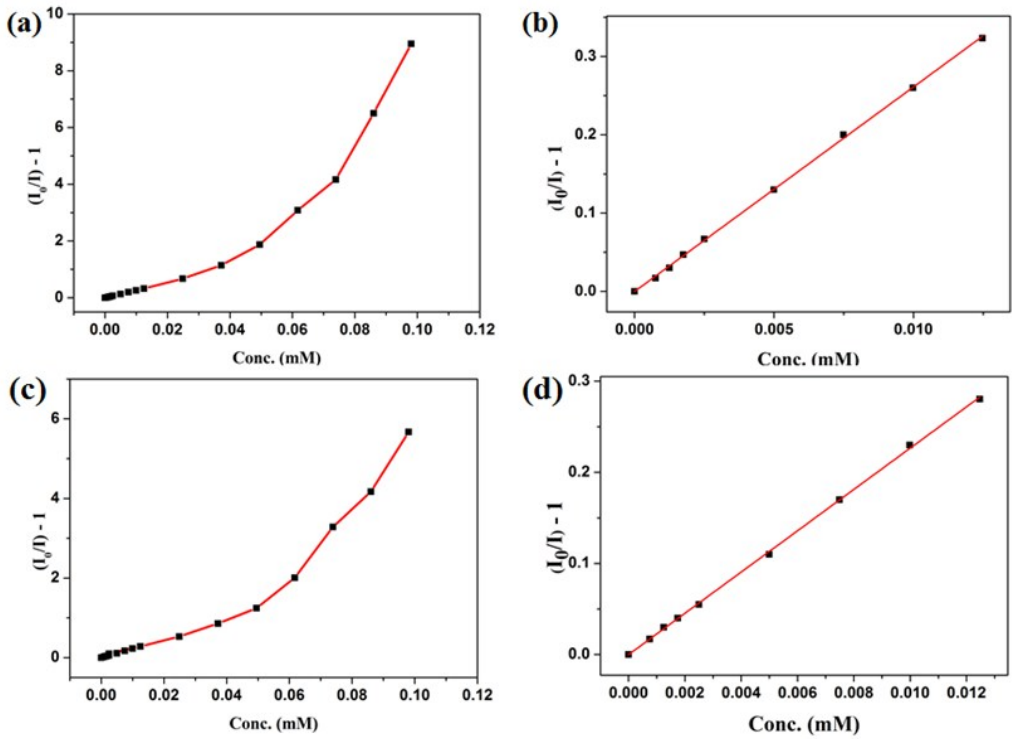

Fig. S11 SV curves for **(a) 1** and (c) **2** by gradual addition of $Cr_2O_7^{2-}$ ion (40 μL, 5 × 10^{-3} M) in DMF. Emission quenching linearity relationship at low concentrations of $Cr_2O_7^{2-}$ ion for **(b) 1** and (d) **2**.

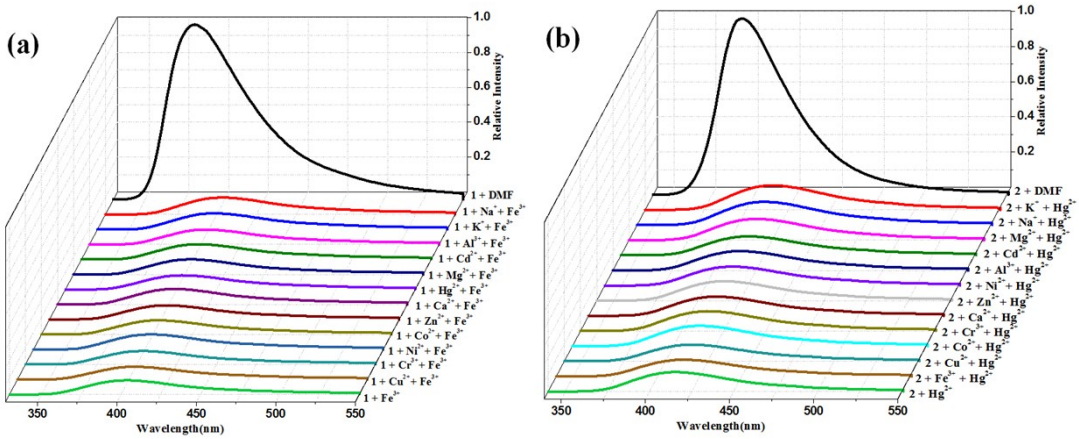

Fig. S12 The relative emission intensity of (a) **1** and (b) **2** before and after addition Fe^{3+} ion (50 μL, 5 × 10^{-3} M) and other metal ions (50 μL, 5 × 10^{-3} M).

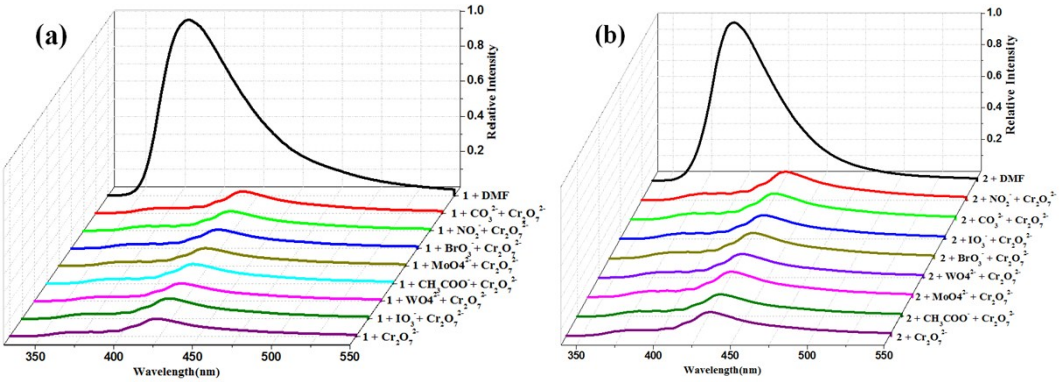

Fig. S13 The relative emission intensity of (a) **1** and (b) **2** before and after addition $Cr_2O_4^{2-}$ ion (40 μL, 5 × 10^{-3} M) and other anions (40 μL, 5 × 10^{-3} M).

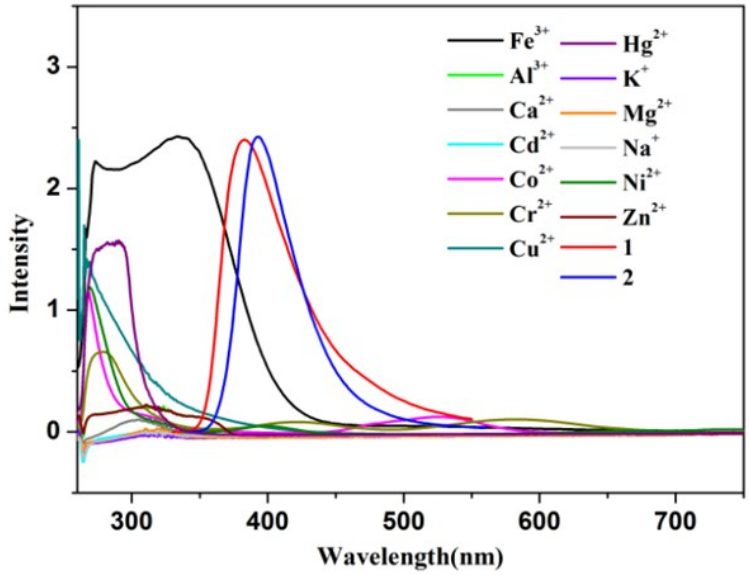

Fig. S14 Spectral overlap between UV-vis absorbance spectra of metal ions and luminescence emission spectra of MOFs **1** and **2** in DMF.

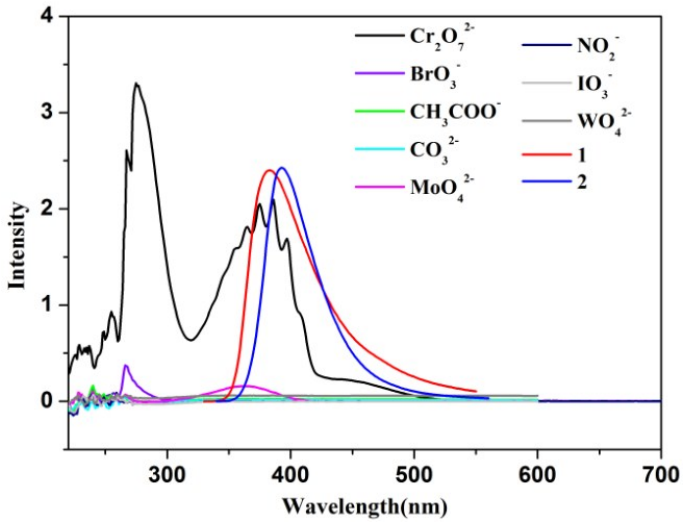

Fig. S15 Spectral overlap between UV-vis absorbance spectra of inorganic anions and luminescence emission spectra of MOFs **1** and **2** in DMF.

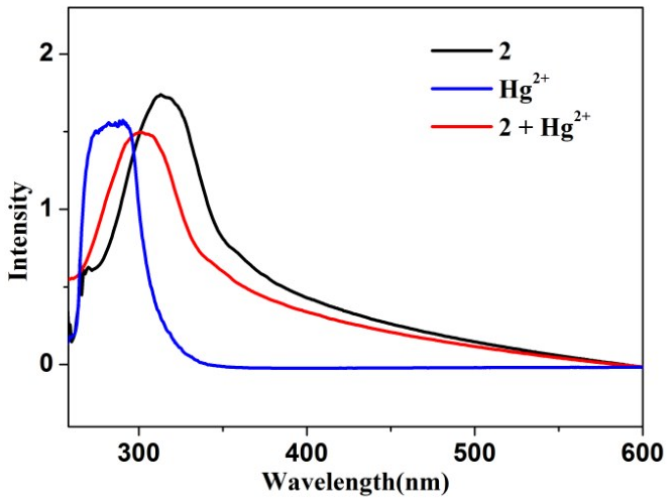

Fig. S16 UV−vis spectra of **2** before and after addition of Hg^{2+} ion.

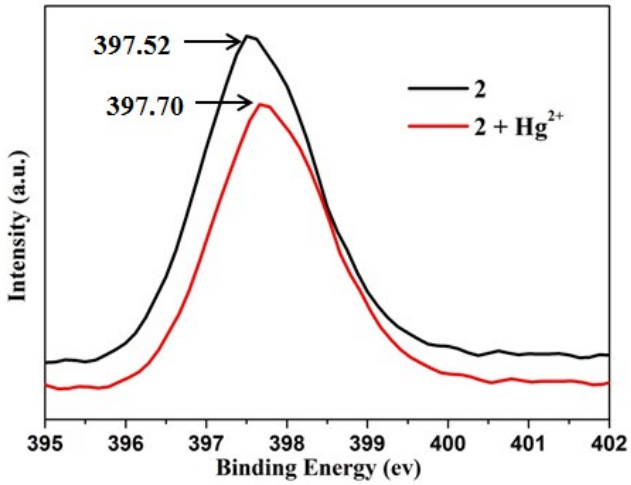

Fig. S17 N 1s XPS spectra of **2** before and after immersed in Hg^{2+} ion.

Table S4. The ICP results of MOF **2** before and after treated with Hg^{2+} ion for 12 hours.

MOF **2**	concentration /μM
Initial value / Hg^{2+}	0.75
After treated with Hg^{2+} for 12 hours/ Hg^{2+}	0.36

Table S5. The quenching constant or detection limit table of selected MOFs materials for Fe^{3+}, Hg^{2+} and $Cr_2O_7^{2-}$ ions.

MOFs	Ions	Detection limit / (M)	Quenching constant / (M^{-1})	Ref
1	Fe^{3+}	1.1×10^{-7}	1.32×10^4	Our work
	$Cr_2O_7^{2-}$	6.9×10^{-8}	1.98×10^4	
2	Hg^{2+}	1.2×10^{-7}	1.27×10^4	
	$Cr_2O_7^{2-}$	9.1×10^{-8}	1.77×10^4	
$\{[Eu(L)(BPDC)_{1/2}(NO_3)]\cdot H_3O\}_n$	Fe^{3+}		5.16×10^4	3
$\{[Tb(L)(BPDC)_{1/2}(NO_3)]\cdot H_3O\}_n$			4.30×10^4	
$\{[Zn_3(bpydb)_2(atz)_2(DMF)](DMF)_6\}_n$	Fe^{3+}		1.15×10^4	4
Tb-DSOA	Fe^{3+}		3.54×10^3	5
$[Cd_3\{Ir(ppy\text{-}COO)_3\}_2(DMF)_2(H_2O)_4]\cdot 6H_2O\cdot 2DMF$	Fe^{3+}		1.17×10^4	6
	$Cr_2O_7^{2-}$		3.48×10^4	
$\{[Cd(BIPA)(IPA)]\cdot DMF\}_n$	Hg^{2+}	5.0×10^{-7}	9.21×10^3	7
$\{[Cd(BIPA)(HIPA)]\cdot DMF\}_n$		2.5×10^{-7}	1.28×10^4	
TMU-34(-2H) in water	Hg^{2+}	1.8×10^{-6}	3.73×10^3	8
$[TbL_{1.5}(H_2O)_2]\cdot H_2O$	Hg^{2+}		7.46×10^3	9
$[Zn(2\text{-}NH_2bdc)(bibp)]_n$	Hg^{2+}	4.2×10^{-8}	4.55×10^3	10
UiO-66@Butyne	Hg^{2+}	1.1×10^{-8}		11
$[Eu_2(tpbpc)_4\cdot CO_3\cdot H_2O]\cdot DMF\cdot solvent$	$Cr_2O_7^{2-}$	1.1×10^{-6}	1.0×10^4	12
$\{[Zn_2(tpeb)_2(2,3\text{-}ndc)_2]\cdot H_2O\}_n$	$Cr_2O_7^{2-}$	1.7 ppb	7.3×10^4	13

References

(1) Bruker 2000, SMART (Version 5.0), SAINT–plus (Version 6), SHELXTL (Version 6.1), and SADABS (Version 2.03); Bruker AXS Inc.: Madison, WI.

(2) G. M. Sheldrick, Crystal structure refinement with SHELXL, *Acta Cryst.*, 2015, **C71**, 3−8.

(3) W. Yan, C. L. Zhang, S. G. Chen, L. J. Han, H. G. Zheng, *ACS Appl. Mater. Interfaces*, 2017, **9**, 1629−1634.

(4) M.-Y. Sun, D.-M. Chen, *Polyhedron*, 2018, **147**, 80−85.

(5) X.-Y. Dong, R. Wang, J.-Z. Wang, S.-Q. Zang, T. C. W. Mak, *J. Mater. Chem. A*, 2015, **3**, 641−647.

(6) K. Fan, S.-S. Bao, W.-X. Nie, C.-H. Liao, L.-M. Zheng, *Inorg. Chem.*, 2018, **57**, 1079−1089.

(7) Z. J. Wang, L. J. Han, X. J. Gao, H. G. Zheng, *Inorg. Chem.,* 2018, **57**, 5232−5239.

(8) S. A. A. Razavi, M. Y. Masoomi, Ali. Morsali, *Inorg. Chem*., 2017, **56**, 9646−9652.

(9) H.-M. Wang, Y.-Y. Yang, C.-H. Zeng, T.-S. Chu, Y.-M. Zhu, S. W. Ng, *Photochem. Photobiol. Sci.,* 2013, **12**, 1700−1706.

(10) L. Wen, X. Zheng, K. Lv, C. Wang, X. Xu, *Inorg. Chem*., 2015, **54**, 7133−7135.

(11) P. Samanta, A. V. Desai, S. Sharma, P. Chandra, S. K. Ghosh, *Inorg. Chem.,* 2018, **57**, 2360−2364.

(12) J. Liu, G. Ji, J. Xiao, Z. Liu, *Inorg. Chem.,* 2017, **56**, 4197−4205.

(13) T.-Y. Gu, M. Dai, D. J. Young, Z.-G. Ren, J.-P. Lang, *Inorg. Chem.,* 2017, **56**, 4668−4678.